INSTITUTE OF PHYSICS PUBLISHING JOURNAL OF PHYSICS D: APPLIED PHYSICS
J. Phys. D: Appl. Phys. **37** (2004) 2996–2999 PII: S0022-3727(04)75243-2

Electron avalanche sliding along a dielectric surface

A Shvydky, V P Nagorny and V N Khudik

Plasma Dynamics, Corp., 417 E. 8 Mile Rd, Hazel Park, MI 48030, USA

E-mail: ashvydky@plasmadynamics.com

Received 25 January 2004, in final form 27 July 2004
Published 8 October 2004
Online at stacks.iop.org/JPhysD/37/2996
doi:10.1088/0022-3727/37/21/009

Abstract
We consider the dynamics of an electron avalanche propagating along a dielectric surface in a channel wherein the Townsend breakdown condition does not hold. We show that when the angle θ between the electric field and the channel wall is less than some critical value θ_{cr}, the electron avalanche grows. The function $\theta_{cr} = \theta_{cr}(E)$ is found by kinetic Monte-Carlo simulations for a mixture of Xe and Ne gasses.

1. Introduction

In barrier discharges, along with the commonly known volume discharge phenomena, there also exist a variety of phenomena pertinent to the dielectric surface (e.g. expansion of the ionization region along the dielectric above the cathode and the anode in micro-discharges, which is exploited in plasma display panels (PDPs) [1, 2]). Among them the propagation of an electron avalanche near the dielectric surface is of considerable interest.

The phenomenon studied in this short paper was observed during the numerical simulation of reset discharges that are used to bring all cells in a PDP to the same state [3,4]. In these discharges, the voltage applied to one of the electrodes is slowly increased at the rate of several volts per microsecond; at the same time the charge collected on the dielectric layers in each cell counteracts the increase in the voltage across the discharge gap, so that all the cells are effectively kept near the breakdown. It was noticed that, in some circumstances, the maximum of the charge density in the cell was unexpectedly far away from the electric field lines along which the balance between the ion production and ion losses is positive:

$$\gamma\left[\exp\left(\int \alpha\,\mathrm{d}x\right) - 1\right] - 1 \geqslant 0, \qquad (1)$$

where α is the Townsend ionization coefficient, γ the secondary electron emission coefficient, and the integral is taken over the electric field line (we recall that at breakdown the left-hand side of this equation is equal to zero). It turned out that, although the geometry of the electric field in the multi-electrode PDP cell is quite intricate (to a great extent, due to the charges on the dielectric walls), the mechanism responsible for this puzzling discharge behaviour is very simple and based on elementary processes: electron impact ionization, drift, and diffusion.

It appears at first sight that when the swarm of electrons drifts in the volume surrounded by the dielectric walls, electron diffusion can only increase the losses of the particles to the walls, and doing so makes the avalanche weaker. We will see below that in some cases the diffusion can work in the opposite way—it can contribute to the very existence of the electron avalanche.

To avoid geometrical complications, we consider avalanche propagation in the plane channel with dielectric walls (see figure 1), filled with a noble gas (or a mixture of noble gases). We suppose that there is a homogeneous electric field $\vec{E}$ in the channel that crosses the channel walls at an angle θ. To distinguish the phenomenon studied from Townsend breakdown between the walls of the channel, we suppose that

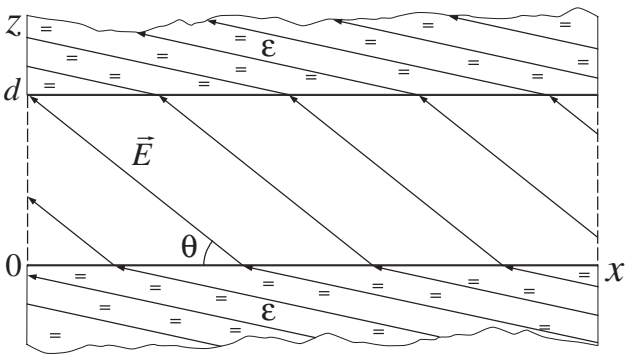

Figure 1. Channel (slit) inside the dielectric slab with oblique electric field lines.

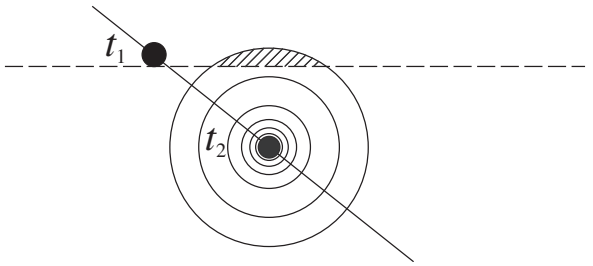

Figure 2. The density in the electron swarm at consecutive moments of time.

the secondary electron emission coefficient of the dielectric surface $\gamma = 0$, so that the condition (1) is certainly not satisfied.

If electron diffusion is negligible, electron avalanche propagation is reduced to a simple motion of the electron swarm with a constant velocity v_e along the electric field line. The number of electrons in the swarm grows as it moves away from the upper wall of the channel. When the electrons reach the lower wall, they are all absorbed by the wall and the avalanche disappears.

The process of electron diffusion can change the picture dramatically. Now, due to the diffusion, the electron swarm increases in size as it moves along the electric field (see figure 2) and some portion of the electrons (dashed area in the figure) may still remain at the same initial distance from the lower wall of the channel. If the rate of electron production r is large enough, this portion can even grow with time! So, although the electrons are continuously taken up by the dielectric surface, newborn electrons replace them, and the electron avalanche continues to move along the surface and grow with time. When the channel is long enough, the amount of charge produced in the near-surface avalanche by a single initial electron can exceed by many times that produced in the avalanche along the electric field line.

2. Fluid model

In this section, we will study the electron avalanche propagation in the framework of the fluid model (see, e.g. [5]), in which the continuity equations for electrons and ions are coupled with the Poisson equation:

$$\frac{\partial}{\partial t} n_e + \operatorname{div}\left[-n_e \mu_e \vec{E} - D_e \nabla n_e\right] = r n_e, \tag{2}$$

$$\frac{\partial}{\partial t} n_i + \operatorname{div}\left[n_i \mu_i \vec{E}\right] = r n_e, \tag{3}$$

$$\operatorname{div} \vec{E} = \frac{e}{\epsilon_0}(n_i - n_e), \tag{4}$$

where n_e and n_i are the electron and ion densities, μ_e and μ_i are the electron and ion mobilities, D_e is the electron diffusion coefficient, r the electron impact-ionization rate, e the unit charge, and ϵ_0 the vacuum permittivity. Note that in the local-field approximation, the electron transport coefficients, and the ionization rate are functions of the electric field. We neglect the processes of recombination, photo-ionization and photoemission. Since we also neglect the secondary electron emission from the channel wall caused by ions bombarding the dielectric surface, the boundary conditions for electrons in the simplest form can be written as[1]

$$n_e|_{z=0} = 0, \qquad n_e|_{z=d} = 0. \tag{5}$$

In the early stage of the electron avalanche development (as long as the charge created in the channel is small and does not affect the electric field), the ions do not influence the motion of the electrons at all.

First, let us consider the case where the electron avalanche propagates as a near-surface wave wherein the electron density does not change along the channel (i.e. along the x-axis, see figure 1). Equation (2) takes the form

$$\frac{\partial}{\partial t} n_e + \frac{\partial}{\partial z}\left[n_e v_z - D_e \frac{\partial}{\partial z} n_e\right] = r n_e, \tag{6}$$

where $v_z = -\mu_e E_z$. While the electric field is constant, $\vec{E} = \text{const}$, we can easily solve equation (6). After substituting $n_e \propto \mathrm{e}^{\nu t}$ and using boundary conditions (5), from equation (6) we find the spatial distribution of the electron density in the near-surface wave and its growth (damping) rate:

$$n_e \propto \mathrm{e}^{\nu t} \sin\left(\frac{\pi z}{d}\right) \mathrm{e}^{-z \sin\theta / l}, \tag{7}$$

$$\nu = r - \frac{v_z^2}{4 D_e} - \frac{\pi^2 D_e}{d^2}, \tag{8}$$

where

$$l = \frac{2 D_e}{\mu_e |E|} \tag{9}$$

is the diffusion length, which characterizes the localization size of the wave in the z-direction. So, in the fluid model, only two hydrodynamic parameters—the electron diffusion coefficient and the electron mobility—influence the spatial profile of the wave, whereas the third parameter, namely the ionization rate, affects only the increment (decrement) of the wave growth (decay).

When the size of the wave localization is much smaller than the channel width, $l/\sin\theta \ll d$, equations (7) and (8) take the form

$$n_e \propto \mathrm{e}^{\nu t} z\, \mathrm{e}^{-z \sin\theta / l}, \tag{10}$$

$$\nu = r - \frac{v_z^2}{4 D_e}. \tag{11}$$

In accord with the qualitative consideration of the previous section, in wide channels, the growth rate increases with increase in the electron diffusion coefficient.

From equation (2), one can easily find the spatial distribution of the electron density in the avalanche initiated by a single electron. Keeping the same spatial profile in the z-direction, the electron swarm moves with the constant velocity $v_x = -\mu_e E_x$ in the x-direction and expands along the dielectric surface:

$$n_e = N_e(t) \psi_1(x, y, t) \psi_2(z), \tag{12}$$

$$\psi_1(x, y, t) \equiv \frac{1}{4\pi D_e t} \exp\left[-\frac{[x - v_x t]^2 + y^2}{4 D_e t}\right], \tag{13}$$

$$\psi_2(z) \equiv \frac{\pi^2 l^2 + d^2 \sin^2\theta}{\pi l^2 d (1 + \mathrm{e}^{-d \sin\theta / l})} \sin\left(\frac{\pi z}{d}\right) \mathrm{e}^{-z \sin\theta / l}, \tag{14}$$

[1] Use of more accurate boundary conditions $D_e \partial n_e / \partial x = -(1/4) v_{\mathrm{th}} n_e$, where v_{th} is the electron thermal velocity, would only complicate the analytical formulae without significantly changing the results.

where $N_e(t) = e^{\nu t}$ is the number of electrons in the avalanche. The total amount of charge produced by the avalanche till the moment t is given by

$$Q(t) = e\left(\frac{r}{\nu}\right)(e^{\nu t} - 1). \tag{15}$$

The critical value of the angle θ_{cr} when the avalanche is not damped can be found from the condition $\nu = 0$:

$$\sin\theta_{cr} = \sqrt{\frac{4D_e r(E)}{\mu_e^2 E^2}}. \tag{16}$$

Note first that the electron avalanche is always damped when the electric field is normal to the dielectric surface; therefore, the hydrodynamic parameters (when the fluid model is applicable) must meet the condition

$$\frac{4D_e r(E)}{\mu_e^2 E^2} < 1. \tag{17}$$

Second, if the anisotropy of the electron diffusion is taken into account (the longitudinal and transverse diffusion coefficients are different), one must use the following expression for D_e in equations (8), (9) and (16):

$$D_e = D_L \sin^2\theta + D_T \cos^2\theta. \tag{18}$$

3. Kinetic Monte-Carlo simulations

A more accurate and complete description of the propagation of the electron avalanche near the dielectric surface can be obtained from kinetic Monte-Carlo simulations. Using cross sections of elastic and inelastic (excitation and ionization) collisions of electrons with neutral atoms from [6], we have performed these simulations in a channel filled with the gas mixture composed of 7% Xe and 93% Ne (which is often used in PDPs) under a pressure $P = 500$ Torr. The channel width is assumed to be so great that the upper channel wall does not influence the near-surface avalanche. Since the spatial charge and the charge deposited on the dielectric surface are always small, the electric field $\vec{E}$ is a constant within the channel.

In our numerical experiments, one seed electron, placed at the moment $t = t_0$ at a distance z_0 from the lower channel wall ($t_0 = 0$ and $z_0 = 0.017$ cm in figure 3), initiates the electron avalanche. The avalanche 'touches' the dielectric surface at the moment $t = t_1$ ($t_1 = 0.6$ ns in figure 3) and after some transient process it transforms into the near-surface avalanche (approximately at the moment $t_2 = 2.5$ ns in figure 3). Later, if $\theta = \theta_{cr}$, the number of electrons in the avalanche only fluctuates with time (due to the statistical nature of the ionization processes); if θ is smaller (greater) than θ_{cr}, the number of electrons increases (decreases) with time.

Figure 4 compares the results from the kinetic simulations with those obtained from the fluid model (note that the transport coefficients μ_e, D_L, D_T, and the ionization rate r in this model have been found as 'swarm' parameters [7, 8] using the same kinetic code). As one can expect, the difference between the kinetic and hydrodynamic descriptions gradually increases with increase in the electric field.

In the region $E/N \lesssim 100$ Td, where energy losses of the electrons due to elastic and excitation collisions dominate,

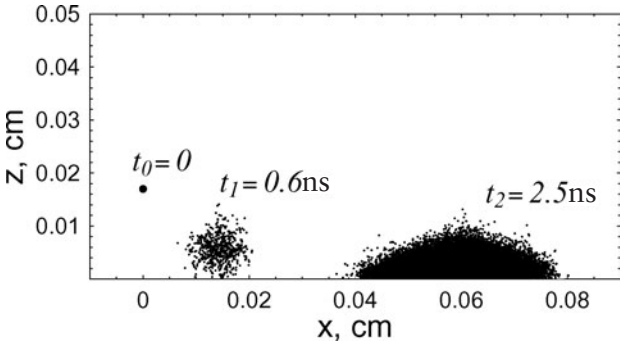

Figure 3. Propagation of the electron avalanche near the dielectric surface; $E/N = 100$ Td and $\theta = \theta_{cr} \approx 35^\circ$.

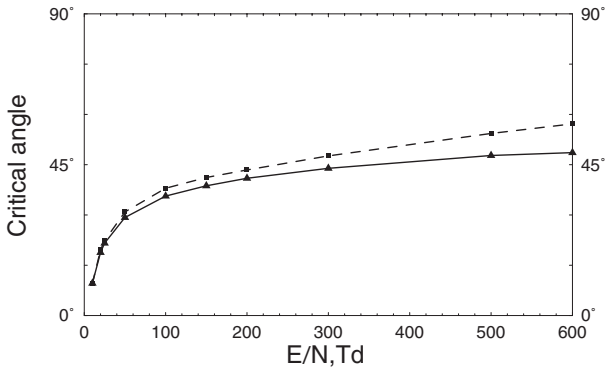

Figure 4. Critical angle at different values of the electric field, from kinetic simulations (——) and from the fluid model (- - - -).

the function $\theta_{cr}(E)$ grows fairly quickly. At greater values of the electric field, where energy losses of the electrons are determined mainly by ionization collisions, this function changes quite slowly (e.g. $\theta_{cr}(600\,\text{Td}) - \theta_{cr}(300\,\text{Td}) < 5^\circ$!).

The remarkable feature of the function $\theta_{cr}(E)$ is that it is weakly sensitive to the properties of the dielectric surface. For example, when in our kinetic simulations, instead of a fully-absorbing wall, we take a semi-mirror wall, which absorbs half of the falling electrons and reflects the other half, the distribution of electrons near the surface changes significantly (especially at large values of the electric field, see figure 5); but the critical angle increases by less than 1% (for $E/N \leqslant 600$ Td)!

As one can also see from figure 5, the characteristic size of the avalanche in the direction normal to the dielectric surface significantly decreases with increase in the electric field.

4. Conclusion

Due to the diffusion processes, the electron avalanche can propagate near the dielectric surface even when the electric field lines cross this surface. For crossing angles $\theta < \theta_{cr}$, the electron swarm grows exponentially with time and expands along the dielectric surface; it has the same characteristic size in the direction normal to the surface all the way along the channel. Note that this phenomenon does not exist above metal surfaces, since the electric field is always normal to them.

The kinetic simulations show that the critical angle θ_{cr} changes quickly at small E and slowly increases at large

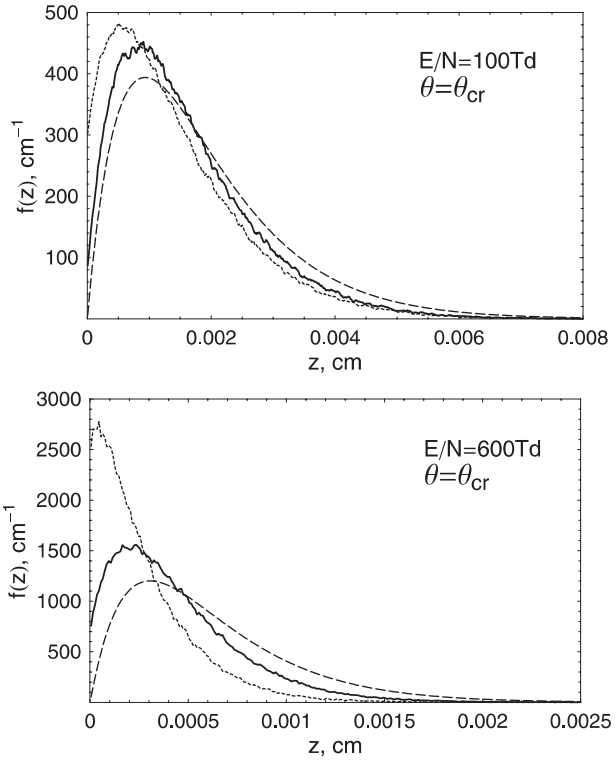

Figure 5. Spatial distribution function of electrons near the surface: (——): fully-absorbed wall; (- - - -): semi-mirror wall; (– – –): fluid model. The function $f(z)$ is defined as $f(z) = \int n_e \, \mathrm{d}x \, \mathrm{d}y / \int n_e \, \mathrm{d}x \, \mathrm{d}y \, \mathrm{d}z$.

electric fields; it depends very weakly on the absorbing/reflecting properties of the dielectric surface.

Note that our discussion can be readily generalized to the case when the electric field is not homogeneous and the angle θ changes within the channel: the avalanche will always grow with time if θ does not exceeds θ_{cr} at all points of the dielectric surface. (And, since this phenomenon also exists in the cylindrical channel, it can, apparently, manifest itself at the breakdown of curved lamps of some geometrical configurations.)

When the channel is long enough, then, somewhere along the channel the avalanche generates a charge large enough to affect the electric field. Further development of the discharge (at the nonlinear stage) depends on the specifics of a particular device and a discussion of this is beyond the scope of this paper. We only note that the charge deposited on the dielectric walls can redirect the electric field lines along the channel (similar to [9,10]), increasing the charge production within the channel.

While, generally, a barrier discharge is determined to a large extent by such processes as secondary electron emission and charge deposition on dielectric walls, we believe that the sliding avalanche can appear, as a fragment, in various types of discharges, as long as a dielectric surface and an oblique electric field are present.

References

[1] Schermerhorn J D, Anderson E, Levison D, Hammon C, Kim J S, Park B Y, Ryu J H, Shvydky A and Sebastian A 2000 *SID 00 Digest* **31** 106–9
[2] Boeuf J P 2003 *J. Phys. D: Appl. Phys.* **36** R53–79
[3] Weber L 1998 *US Patent* 5745086
[4] Tsai-Fu Wu, Chien-Chih Chen, Chien-Chou Chen and Wen-Fa Hsu 2003 *IEEE Trans. Plasma Sci.* **31** 272–80
[5] Raizer Yu P 1991 *Gas Discharge Physics* (Berlin: Springer)
[6] SIGLO DataBase, http://www.siglo-kinema.com/database/xsect/siglo.sec
[7] Sakai Y, Tagashira H and Sakamoto S 1977 *J. Phys. D: Appl. Phys.* **10** 1035–49
[8] Blevin H A, Fletcher J and Hunter S R 1978 *J. Phys. D: Appl. Phys.* **11** 1653–65
[9] Brok W J M, van Dijk J, Bowden M D, van der Mullen J J A M and Kroesen G M W 2003 *J. Phys. D: Appl. Phys.* **36** 1967–79
[10] Nedospasov A V and Novik A E 1961 *Sov. Phys.—Tech. Phys.* **5** 1261–7